

Fire Retardancy of Polymers: New Strategies and Mechanisms, Edited by T.R. Hull and B.K. Kandola, p 168-183, Royal Society of Chemistry, Cambridge, UK, 2009.

Study of the Relationship Between Flammability and Melt Rheological Properties of Flame Retarded Poly(Butylene Terephthalate) Containing Nanoclays

*S. Nazare**,¹*T. R. Hull*,²*B. Biswas*,¹*F. Samyn*,³*S. Bourbigot*,³*C. Jama*,³*A. Castrovinci*,⁴*A. Fina*⁴,
*G. Camino*⁴

¹ Centre for Materials Research and Innovation, University of Bolton, Deane Campus, Bolton, BL3 5AB (U.K)

² Centre for Fire Hazards Science, University of Central Lancashire, Preston, PR1 2HE (UK)

³ Procédés d'Elaboration de Revêtements Fonctionnels (PERF), LSPES, UMR-CNRS 8008, ENSCL, BP 90108, 59650 Villeneuve d'Ascq, (France)

⁴ Politecnico di Torino Sede di Alessandria-Centro di Cultura per l'Ingegneria delle Materie Plastiche Viale Teresa Michel 5 15100 Alessandria (Italy)

The influence of melt rheological properties on the burning behaviour of multi-component polymer formulations containing flame retardant micro-particles and inorganic nanoclays has been investigated. Two types of nanoclays with different shape, size, structure, and organic surface treatments with and without flame retardant additive have been used to prepare flame retarded poly(butylene terephthalate) (PBT) composites. Melt rheology and differential scanning

calorimetry has been used to study nanocomposite morphology and crystallinity of such multi-component polymer formulations. Melt viscosity as a function of temperature have also been measured to study processes taking place during heating. Thermogravimetry and cone calorimetry at 50 kW/m² heat flux has been carried out to study thermal stability and flammability respectively.

Rheological studies suggest that PBT formulations containing two types of nanoclays with different shape, size and structure result in PBT nanocomposites with diverse morphologies. Calorimetric studies have shown that nanocomposites with different morphologies have polymer chains with different mobility, thus affecting melting and crystallisation behaviour. Thermal analysis, however, suggests that despite changes in melt viscosities, PBTs containing the two different clays do not show significant differences in thermal decomposition behaviour. Melt viscosity measured as a function of temperature indicates that increased viscosity in the presence of nanoclay prevents dripping and flowing of the polymer. Furthermore, the fire behaviour is influenced by changed melt rheological behaviour of polymer composites such that the increased melt viscosity shortens the time to ignition but significantly reduces heat release rate, as measured by cone calorimetry.

Keywords: Nanocomposites, Flame retardancy, Melt rheology and Burning behaviour

1. Introduction

Recent studies on a new class of flame retardant system containing nanoclay and conventional flame retardant microparticles have shown that the threshold concentration of flame retardant required to achieve acceptable levels of flame retardancy can be significantly reduced in the presence of nanoclay. Bourbigot et al¹ have observed synergistic effects while incorporating nanofillers into intumescent formulations. They propose that the reactivity of nanofillers with the intumescent flame retardant modifies the physical behaviour of intumescent char during burning.

In multi-component polymer formulations containing flame retardant micro-particles and inorganic nano particles, research has shown that the structure of the interphase (IP) strongly affects the flame retardancy and mechanical properties of the polymer system.² The formation and structure of the IP is, however, governed by the interaction between solid-solid and solid-liquid phases. Nanoclays with different structural morphologies and organic surface treatments could interact differently with the flame retardant micro-particles, and thus result in materials with distinct physical properties. The structural morphology of the dispersed phase in the polymer strongly affects the rheological properties of the polymer system, which can sequentially alter burning behaviour of the polymer composite.³ Therefore two different nanoclays with different structures have been chosen. Cloisite 30B is a montmorillonite clay modified with a quaternary ammonium salt, which has a layered structure consisting of 2 tetrahedral silicate sheets sandwiching a central octahedral sheet. The aspect ratio of montmorillonite is very high, with a specific surface area of 750m²/g. Sepiolite, also a member

of the same 2:1 phyllosilicate group, is a non-swelling clay with needle-like morphology. Chemically, sepiolite is a microcrystalline-hydrated magnesium silicate with the unit cell formula of $\text{Si}_{12}\text{O}_{30}\text{Mg}_8(\text{OH})_4 \cdot 8\text{H}_2\text{O}$.⁴ The sepiolite structure consists of a magnesium octahedral sheet between two layers of silica tetrahedrons, which extend as a continuous layer with an inversion of the apical ends every six units. This inversion results in the formation of a discontinuous octahedral sheet which allows for the formation of rectangular tunnels growing in the direction of needle axis.⁵ The nanostructured tunnels measure approximately $0.35 \times 1.06 \text{ nm}^2$ in cross section and are filled with zeolitic water. The specific surface area of sepiolite is $(300 \text{ m}^2/\text{g} \pm 10 \text{ m}^2/\text{g})$ and the contact area between the needles are both smaller than the specific surface area and contact area between the clay platelets of montmorillonite. The lower contact area between the needles facilitates dispersion of sepiolite.

Commercially PBT is often rendered flame retardant using halogen-containing additives and a synergist. However, owing to environmental issues, halogenated systems are fast being replaced by additive or reactive flame-retardant systems. Different flame-retardant systems for PBT and thermal decomposition and combustion mechanisms of flame retarded PBT have recently been reviewed by Levchik and Weil.^{6,7} In the present work, interactions between flame-retardant micro-particles and inorganic nano-particles (of different morphologies) dispersed in PBT are examined using rheology, and changes in crystallinity and hence melting behaviour is studied using differential scanning calorimetry. Thermo-analytical studies have been carried out to examine the effect of changed rheology on thermal decomposition of the polymer composites. The viscosity measurements as a function of temperature have been carried out to obtain information about the interactions of the components and the processes taking place during heating. Finally, cone calorimetric experiments have been performed to study the effects of changed melt rheological behaviour on the fire behaviour of PBT formulations.

2. Experimental

2.1. Materials

Polymer- Poly (butyl terephthalate) PBT, Celanex 2000-2 Natur supplied by Ticona;

Nanofiller 1- (CL 30B)- Cloisite 30B, natural montmorillonite modified with methyl, tallow, bis-2-hydroxyethyl, quaternary ammonium chloride (MT2EtOH) (Southern Clay Products, USA);

Nanofiller 2- (SP)- Sepiolite amine, surface modified with benzyl methyl di-hydrogenated tallow ammonium salt. Tolsa, Spain;

Flame Retardant (FR) –Phosphinate salt, Exolit OP1240, Clariant, Germany.

2.2. Sample Preparation

Compounds were prepared by melt blending in a Leistritz ZSE 27 co-rotating intermeshing twin screw extruder. Screw speed was set to 200 rpm and mass flux at 10 kg/h. Screw profile and temperature profile used for compounding PBT materials is shown in Figure 1.

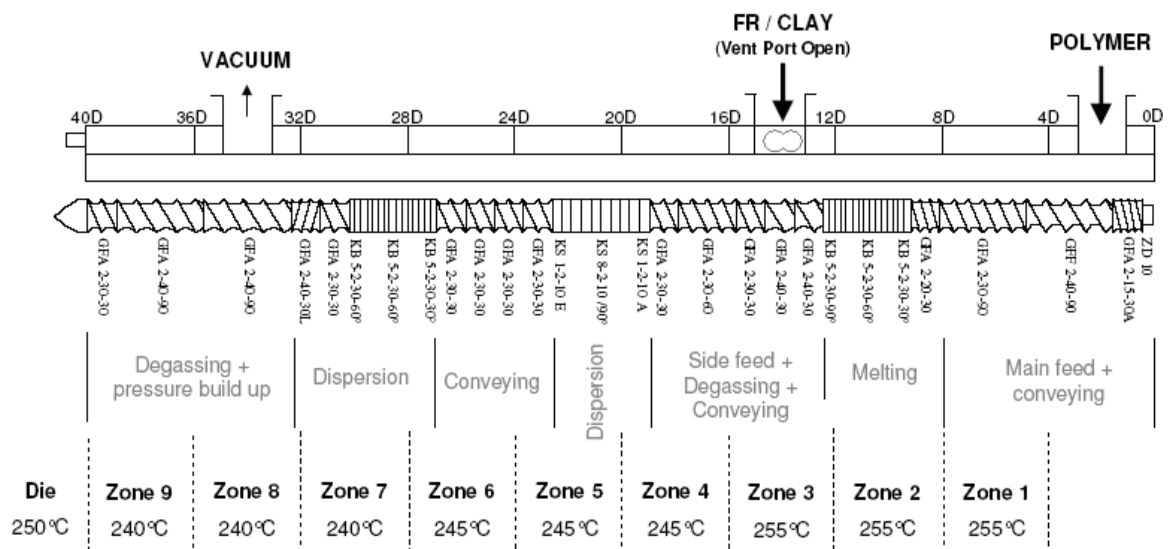


Figure 1: Screw and temperature profile for processing PBT materials.

The polymer was loaded in the main feed and filler added to the molten polymer by means of a gravimetric side feeder. The extruded materials are cooled in water and then pelletised. Samples in the form of powder, films and slabs were prepared for appropriate testing. Sample description and mass percentages of various components in the formulations are given in Table 1.

Table 1. Mass percentages of various components in the formulations

Descriptive codes	Resin (%)	FR (%)	Nanoclay (%)
PBT	100	-	-
PBT+CL 30B	95	-	5
PBT+SP	95	-	5
PBT+FR	82	18	-
PBT+FR+CL 30B	77	18	5
PBT+FR+SP	77	18	5

2.3. Characterisation and Testing

Conventionally, nanocomposite structure(s) in a polymer matrix can be identified by monitoring the position, shape and the intensity of the basal spacing in the lower 2θ region ($2-10^\circ$) of the X-Ray diffractogram. However, the peak in the XRD diffractogram of sepiolite originates from the d-spacing between the sepiolite tunnels and not from the separation between the needles⁴. Therefore, XRD is not a suitable technique to characterise the dispersion of sepiolite in the polymer matrix. Recently, a rheological method has been developed to characterise the nanodispersion of all kinds of platelike, fibrous or dendritic filler materials with high aspect ratios.⁸ This has been used to characterise the nanostructures of the samples in the current study.

A Polymer Laboratories DSC has been used to determine the influence of morphological structure of the nanofillers on the crystallisation behaviour of PBT. The crystallinity (X_c %) for all the samples has been calculated such that:

$$X_c \% = \frac{\Delta H_m}{\Delta H_f} \times 100$$

where ΔH_m is the enthalpy of melting and ΔH_f is enthalpy of fusion.. The theoretical value of ΔH_f for a 100% crystalline PBT has been taken as 140 J/g.⁹

Simultaneous DTA-TGA analysis was performed using an SDT 2960 TA instruments under flowing air (50 ml/min) and at a heating rate of 10 K/min on 10 mg sample masses.

Rheological measurements were carried out on 1 mm thick samples at 240°C using a Dynamic Analyser Rheometer RDA II from Rheometrics. A parallel plate geometry with plate diameter of 25 mm has been used to conduct dynamic frequency sweep experiments. Furthermore, the changes in melt rheological behaviour of polymer composites over a temperature range close to, and above, the degradation temperature have been studied in a nitrogen atmosphere. The samples were heated from 300 to 530°C with a heating rate of 15°C/min. The frequency of oscillation was kept constant at 10 rad/s and the strain amplitude at 10%.

The burning behaviour of PBT formulations has been studied using cone calorimetry (Fire Testing Technology Ltd., UK). 100 x 100 x 6 mm samples were exposed to an incident heat flux of 50 kW/m² under ambient atmosphere.

3. Results and discussion

3.1. Nanodispersion

Viscosity curves for PBT polymer and its composites are shown in Figure 2(a), and a summary of the rheological properties in the low frequency region (at 0.1 rad/s) for all the formulations studied are given in Table 2. In Figure 2(a) PBT shows perfect Newtonian behaviour over all the frequency range measured, giving a shear-thinning component $\eta = 0.02$. Addition of 5% of CL 30B to the polymer matrix shows a shift to non-Newtonian behaviour in the low frequency region and pronounced shear thinning ($\eta = 0.67$) at higher frequencies. A significant increase in the complex viscosity at lower frequencies and pronounced shear thinning in the higher frequency region at low loading levels of 5% w/w is a characteristic feature of intercalated/exfoliated nanocomposite structures.¹⁰ Characterisation of PBT+CL 30B as an intercalated nanocomposite based on its rheological behaviour is in agreement with the XRD results^{11,12} where the characteristic peak of CL 30 B at $2\theta = 4.5^\circ$ corresponding to a d-spacing of 1.88 nm, has moved to lower value of $2\theta = 2.2^\circ$ indicating a d-spacing of 4.0 nm. XRD analyses, confirmed by TEM,^{11,12} show that although the d-spacing has increased, the CL 30B has still maintained its ordered platelet structure to form an intercalated nanocomposite.

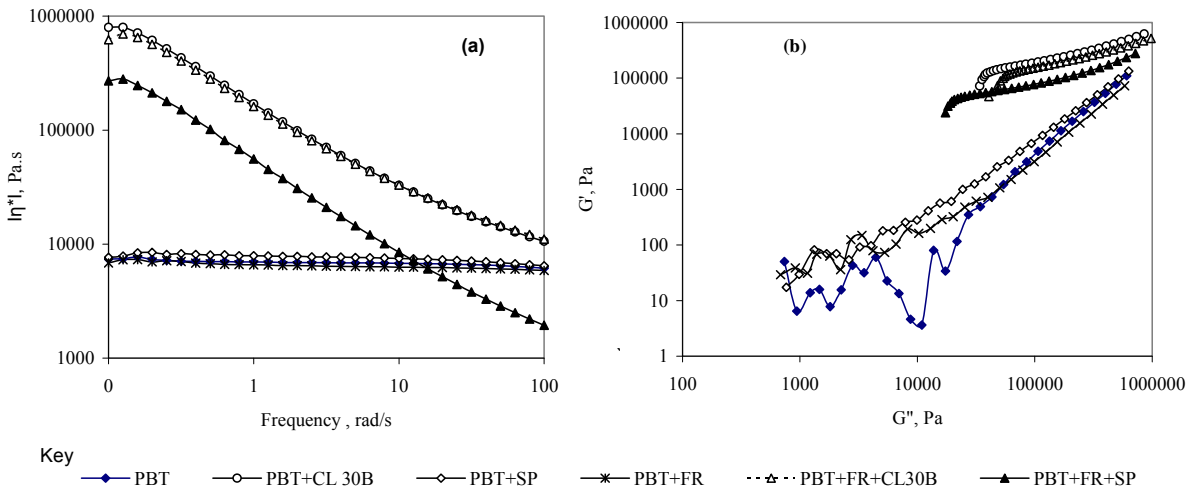


Figure 2: (a) Viscosity versus frequency and (b) G' versus G'' plots for all PBT formulations

In contrast, PBT+SP samples containing 5% w/w of needle-like nanofiller (sepiolite) do not show any change in rheological properties. The viscosity curve in Figure 2(a) for PBT+SP shows perfect Newtonian behaviour similar to that of the pure PBT sample, suggesting that sepiolite remains in tactoid form or does not form a percolated superstructure of well-dispersed nano particles. Lack of confinement of polymer chains by one dimensional needle-like sepiolite particles in PBT+SP samples accounts for the perfect Newtonian behaviour similar to that of pure PBT. Owing to the weak interaction between the sepiolite particles and the PBT polymer, the tethering of polymer chains by sepiolite is not strong enough. Moreover, the change in the yield behaviour of polymer-clay nanocomposite in molten form depends largely on the surface area of the particulates. It is worth noting here that the specific surface area of montmorillonite clay is 750m²/g whereas that of sepiolite can be less than 300m²/g. The higher specific surface area of CL 30B provides greater resistance to polymer chains and hence higher viscosity, especially at lower frequencies. The montmorillonite-based CL 30B forms a classic “card-house” structure. The polymer layered nanocomposite structure is instrumental in imparting solid-like visco-elastic properties to PBT+CL 30B samples.

Table 2 : Rheological properties of PBT formulations at 0.1 rads/s

Samples	$ \eta $, (Pa)	G' , (dyn/cm ²)	G'' , (dyn/cm ²)	Type of composite
PBT	7.4×10^3	6.5×10^0	7.4×10^2	-
PBT+Cl 30B	8.0×10^5	9.4×10^4	9.4×10^4	Intercalated nanocomposite
PBT+SP	7.7×10^2	3.0×10^1	3.0×10^1	Microcomposite
PBT+FR	6.9×10^3	3.9×10^1	3.9×10^1	Microcomposite

PBT+FR+CL 30B	6.2×10^5	7.4×10^4	4.1×10^4	Intercalated nanocomposite
PBT+FR+SP	2.7×10^5	3.1×10^4	3.1×10^4	Intercalated nanocomposite

The rheological properties of PBT+FR in Table 2 do not show substantial change with respect to those of pure PBT, despite 18 % w/w loading of FR. This suggests that addition of micro-particles up to 18 % w/w does not affect the chain movement and hence the rheological behaviour of the polymer system, whereas 5% w/w of nano dispersed clay particles significantly affects rheological properties of the polymer nanocomposite. However, addition of FR to the PBT+SP formulation has resulted in a sizeable increase in the viscosity of the PBT+FR+SP sample and a noticeable increase in the shear thinning at higher frequencies, suggesting that the FR assists in increasing compatibility between polymer chains and sepiolite needles. Sepiolite has a very high concentration of surface silanols spaced every 0.5 nm along the length of needles facilitating coupling reactions with polymer, organic surfactant and/or the flame retardant. This could probably lead to diffusion of small molecules within the sepiolite needles, thereby assisting uniform dispersion of sepiolites within the polymer matrix. Solid-like or pseudo solid-like viscoelastic behaviour of PBT+FR+SP formulation, as seen in Figure 2 and Table 2, can be attributed to enhanced dispersion of sepiolite in the presence of FR . Viscosity values for PBT+CL 30B and PBT+FR+Cl 30B over the whole frequency range tested are comparable (see Table 2), suggesting that the confined structure of CL 30B within the polymer matrix and the chain stiffness of PBT limits further widening of interlayer space in presence of FR. Furthermore, hydroxyl groups in the Cloisite 30B interlayer has two effects on PBT containing carboxyl groups. First, it favours intercalation of PBT chains and the formation of intercalated nanocomposite structure. Second, the enhanced interaction of ammonium cation with the silicate surface is less favourable for replacement of the surface contacts by PBT chains thereby limiting extensive intercalation and further exfoliation of Cloisite 30B in the PBT matrix¹³. The shear thinning behaviour of both the samples containing CL 30B is very similar (see

Figure 2(a)) with shear thinning component of $\eta = 0.67$ for PBT+CL 30B and $\eta = 0.64$ for PBT+FR+CL 30B.

Furthermore, the so called Cole-Cole plots ($\log G'$ versus $\log G''$) in Figure 2(b) may be used to further elucidate the morphological state of such multiphase polymer systems. It can be noted from Figure 2(b) that inclusion of CL 30B in the pristine polymer shows a profound influence on the $\log G'$ versus $\log G''$ plots and hence the morphological state as compared to the pure polymer and flame retarded polymer. Addition of flame retardant to the PBT+SP formulations also shows an upward shift in $\log G'$ versus $\log G''$ plots suggesting a change in the morphological state of the polymer system. Nanodispersion gives rise to a notable increase in the degree of heterogeneity of the polymeric system thereby decreasing the slope of $\log G'$ versus $\log G''$ plots, compared to PBT, PBT+SP and PBT+FR samples. The fact that the $\log G'$ versus $\log G''$ plots in Figure 2(b) differ for different samples suggests that these polymer systems can be regarded as different materials from a rheological point of view.

The frequency-dependent behaviour of storage and loss moduli of a polymer system is also related to its morphological state in molten form. The storage and loss moduli curves plotted as a function of frequency for PBT and its composites are shown in Figure 3. The frequency dependence of storage and loss moduli of PBT, PBT+FR and PBT+SP shown in Fig 3 (a), (c) and (e) suggests that the viscoelastic behaviour of pure polymer is dominated by viscous liquid behaviour (with $G' < G''$ over all the frequency range measured and no cross-over frequency). However, for the sample PBT+Cl 30B (see Figure 3(b)), $G' > G''$ in the lower frequency region suggests solid-like behaviour due to physical jamming of clay platelets. The cross-over frequency is noted at 19.9 rads/s after which the polymer system exhibits viscous liquid behaviour. Addition of FR reduces the cross-over frequency to 6.3 rads/s for the PBT+FR+CL 30B formulation. For PBT+FR+SP formulations, the cross-over frequency is noted at the lower

frequency of 3.2 rads/s indicating that the interaction between needle-like particles of sepiolite and polymer chains is lost at lower shear rates, leading to relaxation of the polymer chains and hence viscous liquid behaviour.

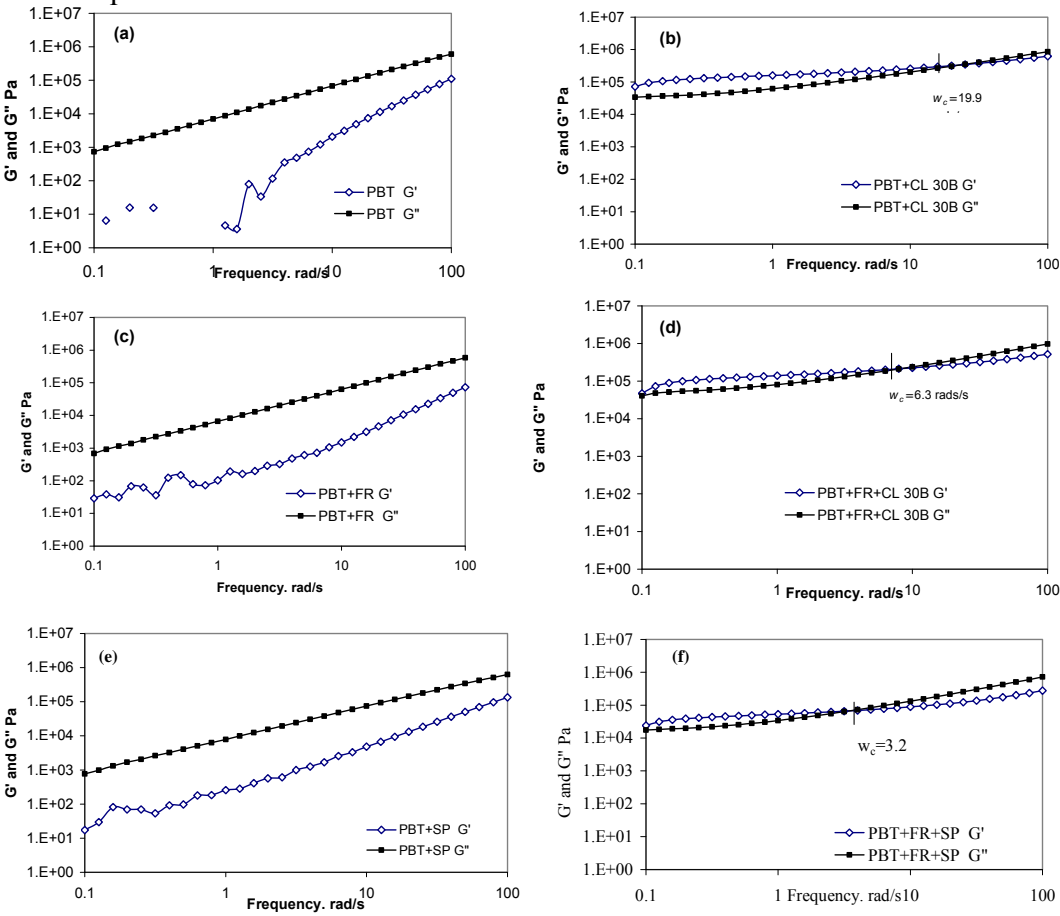


Figure 3: Storage modulus and loss modulus of PBT and its composites

3.2. Differential Scanning Calorimetry and Thermal Analysis

Calorimetric data for pure PBT and normalised (for actual polymer content) calorimetric values for all PBT formulations are given in Table 3. It can be noted that the melting temperatures have remained unchanged. However, the samples containing sepiolite exhibit higher crystallisation temperatures (T_c) compared to those of pure PBT and flame-retarded PBT, both with and without CL 30B. The increased temperature of crystallisation for PBT+SP may be due to the reduced confinement effect from the one dimensional needle-like sepiolite clay particles,

compared to the two dimensional MMT platelets.¹⁴ Furthermore, the crystallisation process starts much earlier in sepiolite-containing samples, but the enthalpy of crystallisation, ΔH_c , is smaller than that of the PBT+CL 30B formulation, suggesting the formation of larger crystals with fewer nucleating sites¹⁵ in the PBT+SP sample. Nanodispersed clay platelets in PBT+CL 30B provide more heterophase nuclei and larger surface area to increase ΔH_c but the triggering of the crystallisation is slightly delayed.¹⁶ Addition of flame-retardant micro-particles reduces the temperature of crystallisation of PBT+FR formulation ($T_c = 190^\circ\text{C}$), compared to that of the pure polymer ($T_c = 195^\circ\text{C}$). Moreover, inclusion of CL 30B in the flame-retarded PBT slightly shifts T_c to a higher temperature, but the enthalpy of crystallisation is still lower than for the PBT+FR sample. On the contrary, addition of sepiolite to the PBT+FR sample significantly increases T_c and ΔH_c of the resulting PBT+FR+SP sample, suggesting early onset of crystallisation in the presence of sepiolite particles. An increase in enthalpy of crystallisation may be explained by improved dispersion of sepiolite particles in the presence of flame-retardant particles, and hence enhanced interaction between sepiolite particles and polymer chains.

Table 3: Calorimetric data for PBT formulations

Samples	$T_m, ^\circ\text{C}$	$T_c, ^\circ\text{C}$	$\Delta H_m, (\text{J/g})$	$\Delta H_c, (\text{J/g})$	$x_c, \%$
PBT	225	195	41	57	29
PBT+Cl 30B	224	193	48	69	35
PBT+SP	224	198	47	62	34
PBT+FR	225	190	43	59	31
PBT+FR+CL 30B	224	193	48	57	34
PBT+FR+SP	225	203	56	65	40

The normalised values for enthalpy of melting recorded during second heating cycles are higher for PBT formulations containing nanofillers, suggesting that greater resistance to melting is

offered by the nanofillers. Enthalpy of melting is highest for the PBT+FR+SP sample (56 J/g) confirming that the sepiolite is nanodispersed in the presence of FR. The percent crystallinity for PBT+FR+SP is the highest of all the samples. The increase in crystallinity can be attributed to nanodispersed sepiolite needles providing heterophase nuclei.

One of the most important property enhancements expected from formation of a polymer nanocomposite is that of thermal stability, either in initial stages or final carbonaceous residues. The degradation of pure PBT in the presence of air proceeds through a free-radical mechanism. The TGA and DTA curves for pure PBT, PBT containing CL 30B and sepiolite SP are shown in Figure 4.

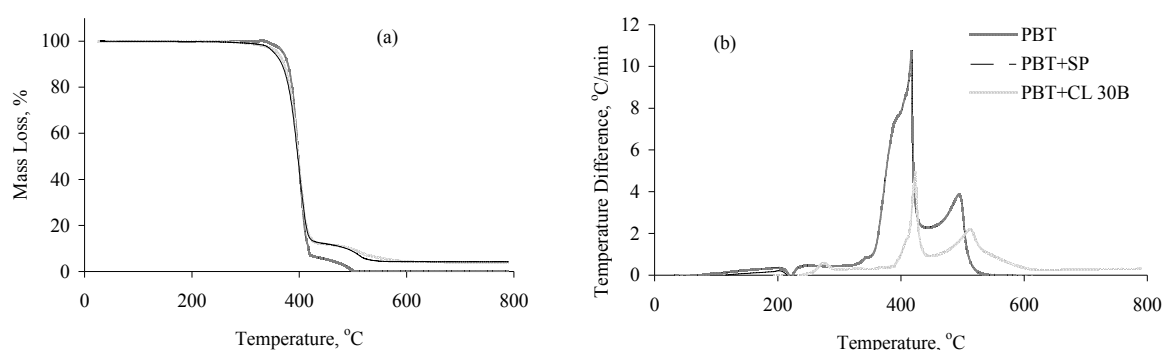


Figure 4: TGA and DTA responses in air for PBT-based materials

The presence of nanoclays has no impact on the thermal stability of PBT below 400°C. Although the clay layers act as a mass-transport barrier to the volatile products generated during decomposition, increasing thermal stability, there are also catalytically active centres in the clay layers, such as those around hydroxyl groups, which might accelerate the decomposition of PBT¹⁶. Both the clays, however improve thermal stability of PBT above 400°C and give rise to similar yields of carbonaceous char at high temperatures. Although the TGA curves for PBT+CL 30B and PBT+SP show a similar trend, the DTA curves are quite different. The small

exothermic peak at 279°C for PBT+CL 30B suggests decomposition of organic modifier, whereas the organic modifier on sepiolite is stable up to 300°C. The DTA curve for PBT+SP shows an exothermic peak at 352°C, which could be due to degradation of the amine group followed by an endotherm that could be attributed to dehydration in which sepiolite loses half of its coordinated water⁵. The main exothermic peak for pure PBT at 417°C, representing release of volatiles, is much smaller in the case of PBT+CL 30B and PBT+SP samples, which probably could be due to the barrier effect of nanoclays. Inclusion of FR in the formulations containing two different clays (not shown here) does not have any synergistic effect on the thermal stability of PBT.

3.3. Melt Viscosity

Viscosity versus temperature curves for PBT-based materials are given in Figure 5. It can be seen from an expanded scale within Figure 5 that the viscosity of neat PBT reduces to near to zero up to 435°C owing to melting and then complete decomposition of the polymer. A sharp increase in viscosity of PBT samples above 435°C can be attributed to the presence of solid carbonaceous residue. Viscosity measurements beyond 435°C for pure PBT have not been possible owing to instrumental limitations. The viscous modulus of the PBT+SP formulation is greater by a factor of 10 compared to that of pure PBT. This increase in viscosity of the PBT+SP formulation over temperature range of 300-415°C, despite a small (5% w/w) loading of SP, is due to reinforcement of the polymer matrix by needle-like nano-particles of sepiolite. However, this effect of adding sepiolite is not seen in the visco-elastic properties measured at 240°C. This suggests that, at higher temperatures, dispersion of sepiolite is improved, resulting in increased viscosity of PBT+SP. However, this increase in viscosity is not sufficient to prevent melt dripping of the sample when exposed to an external heat flux or flame. Above 420°C the viscosity of PBT+SP falls to near zero, owing to degradation of the polymer. A sharp increase in the viscous modulus at 500°C could be attributed to formation of a solid inorganic char. It can

be noted from the inset plot in Figure 5 that the degradation step of PBT+ SP is delayed compared to those of both the pure and flame-retarded PBT. As seen from Figure 5, the increased viscosity of PBT+CL 30B sample, compared to those of the PBT, PBT+SP and PBT+FR formulations over a temperature range of 300-350°C, suggests increased resistance to melt dripping. It is worth noting from Figure5 that, above 350°C, the viscosity for PBT+CL 30B sample does not come close to zero until 425°C, suggesting further resistance to melting over the temperature range 350-425°C.

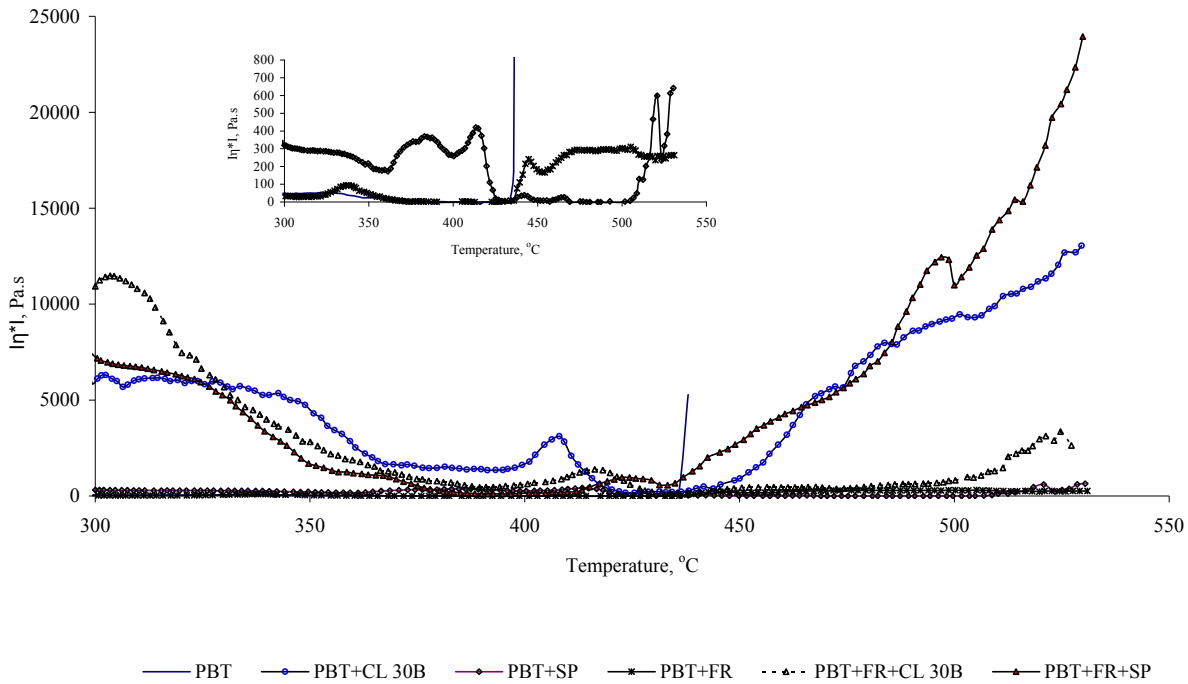


Figure 5: Viscosity versus temperature curves for PBT formulations

Changes in viscosity with increasing temperature for PBT+FR up to 320°C are similar to those in the pure PBT sample. However, at 335°C, a viscosity peak appears which can be assigned to flame-retardant activity in the presence of the P-based intumescent flame retardant. This peak gradually levels to zero around 435°C, which could be due to the formation of phosphoric acid species from the thermal decomposition of the phosphinate. A sharp increase in viscosity and

subsequent stability at higher temperatures for PBT+FR formulation can be attributed to the enhanced formation of char in the presence of the FR.

Finally, addition of 5% w/w of CL 30B and sepiolite (SP) to the PBT+FR formulation, dramatically increases viscosity in the resulting PBT+FR+CL 30B and PBT+FR+SP samples. A gradual decrease in viscosity values of PBT+FR+CL 30B and PBT+FR+SP formulations above 325°C could be due to formation of phosphoric acid species as mentioned earlier. Moreover, the polyphosphoric acid may react with the surfactant of the nanoclay thereby collapsing the nanostructure and thereby resulting in lower viscosity of PBT+FR+CL 30B and PBT+FR+SP. However, the appearance of a shoulder at 360°C (for the PBT+FR+SP formulation) and a viscosity peak at 415°C (for PBT+FR+CL 30B formulation) suggests the formation of a porous carbonaceous char which subsequently collapses, reducing viscosity to near zero in the case of both PBT+FR+SP and PBT+FR+CL 30B. A sharp increase in viscosity of PBT+FR+SP above 410°C may be due to the formation of a char that is reinforced with needle-like nanoparticles.

Addition of CL 30B to PBT+FR has a slightly different effect on viscosity of the resultant formulation than does addition of SP. As seen from Figure 5, the reduction in viscosity is more gradual and prolonged, compared to that of the PBT+FR+SP sample. Owing to the barrier effect of nano-dispersed clay platelets in the polymer matrix, the degradation step of the PBT+FR+CL 30B formulation is delayed compared to that of the PBT+FR+SP formulation. The final charring process starts at 500°C, as opposed to 410°C, for PBT+FR+SP sample. From the above discussion, it can be concluded that PBT+FR+CL 30B formulation might be expected to show the better fire performance owing to increased viscosity and thermal stability in the presence of nanoclay.

3.4. Flammability

The cone data obtained at 50 kW/m² and given in Table 4 shows significant differences for various PBT formulations. Most importantly and of more significance to this work is the time to ignition (TTI). A critical surface temperature for ignition is close to being accepted as a material property, and the time to reach this temperature (TTI) will be a function of the heat transfers.¹⁷

Table 4: Cone calorimetric results at 50 kW/m² heat flux for all PBT formulations.

Sample	TTI (s)	PHRR (kW/m ²)	Avg. HRR* (kW/m ²)	THR* (MJ/m ²)	FIGRA (kW/s)	H _c * (MJ/kg)	Char residue* (%)	CO (g/g)	CO ₂ (g/g)
PBT	64	597	229	138	1.9	22	27	0.26	2.38
PBT+Cl 30B	51	279	177	106	2.1	19	34	0.14	1.85
PBT+SP	44	332	191	115	3.0	21	37	0.13	2.16
PBT+FR	42	250	140	85	1.4	15	32	0.17	1.78
PBT+FR+CL 30B	37	165	110	66	1.3	13	41	0.17	0.84
PBT+FR+SP	40	163	116	70	1.9	16	49	0.21	1.19

Note: * Values at 600 s.

TTI for the neat PBT is greater than the average of the nano- or FR- containing formulations. There are several factors which influence the ignition delay time. However, based on our rheological studies and observations, we propose a hypothesis that an increasing viscosity decreases thermal conductivity essentially by flowing of the molten polymer, and thus results in accumulation of heat at the surface of the sample exposed to an incident heat flux. Furthermore, the thermal properties (kpc) of the solid material are relatively easy to define and measure, but as the rheometric data show, most samples are somewhat molten at their ignition temperature. The increased surface temperature of the sample with higher viscosity means that this sample

reaches ignition temperature more quickly than the sample with low viscosity. Based on this argument, the pure PBT would flow and bubble, allowing the whole sample to reach thermal equilibrium and thus increase the time to ignition. Once the bulk PBT reached the ignition temperature, the burning rate would be more rapid (see Figure 6), giving higher values of PHRR, FIGRA and average HRR, as seen in Table 4. For the samples containing only nanofiller, the reduction in time to ignition can be ascribed to the increased viscosity at the ignition temperature, resulting in higher surface temperature (but a lower bulk temperature).

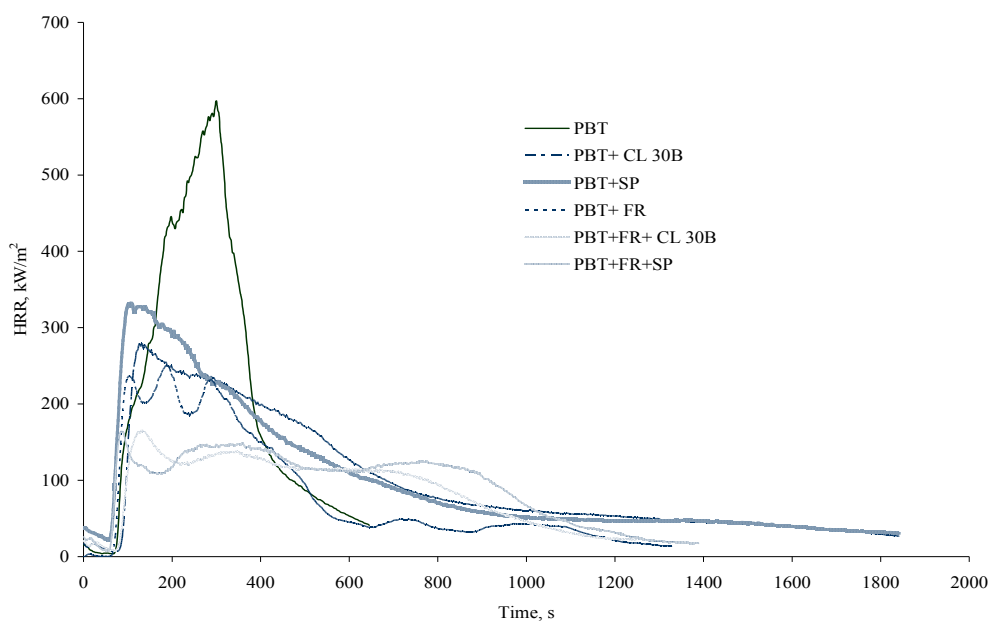


Figure 6: HRR as a function of time for PBT formulations

Comparing the two nanofillers, the sepiolite-containing samples show shorter times to ignition compared to CL 30B-containing formulations. This is in contrast to the above mentioned hypothesis, since the PBT+CL 30B sample with higher viscosity shows increased time to ignition compared to the PBT+SP sample with lower viscosity. The increased time to ignition in PBT+CL30B can be attributed to several other factors including adsorption of volatile products on larger surface areas of clay particles and the barrier effect of the plate-like CL 30B. The early ignition of PBT+SP could also be due to catalytic degradation of the sepiolite amine and/or less efficient barrier properties of sepiolite clay.

With increased viscosity, HRR is decreased to give lower PHRR and lower average HRR. The higher viscosity in the presence of nanoclay may also inhibit the escape of volatile products from the burning polymer into the flaming zone, reducing the HRR. Total heat release values reported at 600 s are also reduced owing to slower burning of samples containing nanofillers.

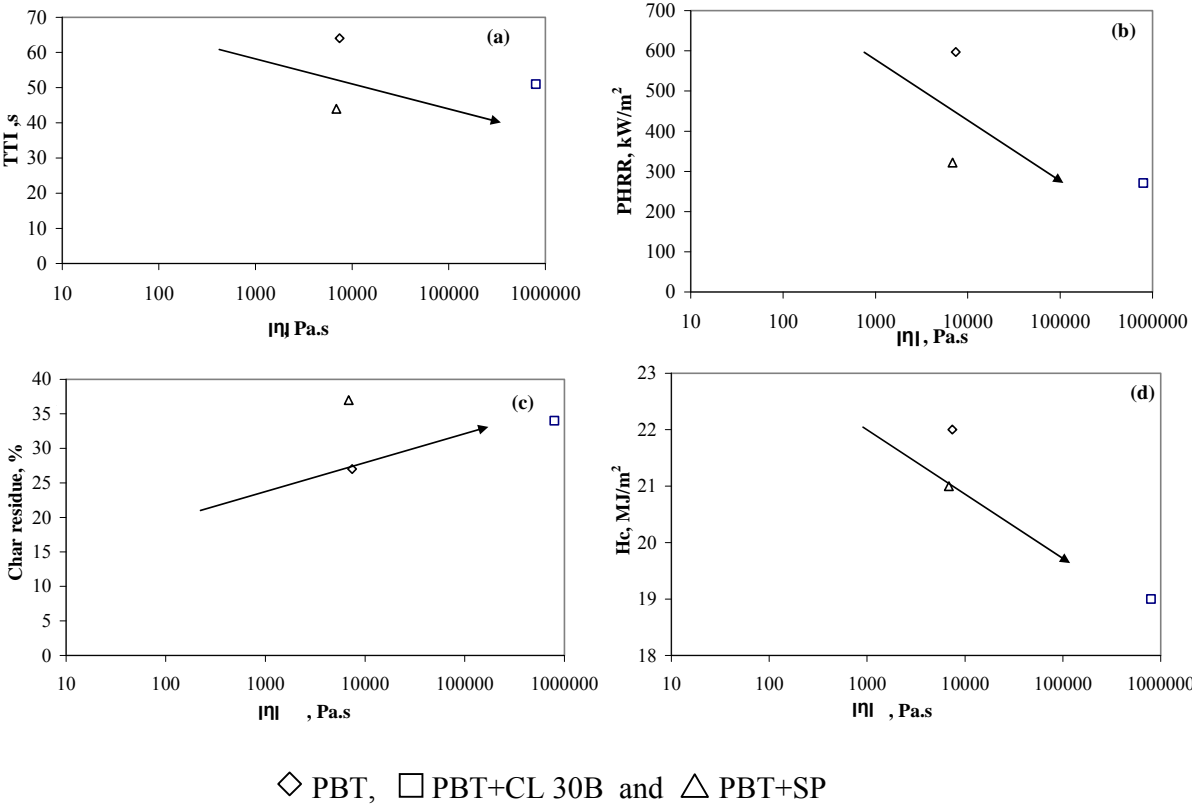


Figure 7: Relationship between (a) TTI, (b) PHRR, (c) char residue and (d) H_c

Furthermore, in order to study the effect of changed rheological properties on the flammability of PBT composites, the relationship between the intrinsic viscosity measured at 300°C and various cone parameters have been plotted in Figure 7. However, to eliminate the additional effect of FR, only PBT, PBT+CL 30B and PBT+SP have been compared. Moreover, the presence of FR would further obscure the effect of changed viscosity on burning behaviour of PBT +FR+ CL 30B and PBT+FR+SP samples. Figure 7 (a) suggests that the time to ignition is related to, viscosity but that other factors, such as nanoparticle morphology or the ability to of nanoparticles to act as a barrier, must also be involved. The peak heat release rate decreases as the viscosity increases, especially between PBT and PBT+SP, but as discussed earlier, the

higher PHRR of PBT may be the consequence of the higher overall temperature of bulk polymer, compared to the higher surface temperature of the nanofilled PBT samples. From Figure 7 (c), it can be seen that the char yield appears to be independent of viscosity, and is probably dependent on the processes occurring in the later stages of burning. Since the char yield does not correlate with the total heat release, this suggests some inconsistencies in the burning behaviour. Furthermore, the modest decrease in heat of combustion with increase in viscosity implies a change in the gas phase oxidation behaviour of the volatile products. Again, this is most likely to be a consequence of the cooler bulk of the nanofilled PBT materials, resulting in incomplete gas-phase combustion, and greater char formation.. In summary, plots in Figure 5 suggest that PBT formulations with higher viscosities exhibit improved post-ignition flame-retardant properties.

4. Conclusions

Rheological measurements suggest that one dimensional needle-like sepiolite has a reduced confinement effect compared to the two dimensional platelets of CL 30B. This results in perfect Newtonian viscous behaviour of PBT+SP melts. This is also confirmed by calorimetric results where PBT+SP samples show higher crystallisation temperature and smaller enthalpy of crystallisation compared to those of PBT+CL 30B, suggesting the formation of larger crystals with fewer nucleating sites.

The FR acts as a compatibiliser and facilitates better dispersion of sepiolite to give higher melt viscosity for PBT+FR+SP formulations in the lower frequency region and pronounced shear thinning at higher frequencies. The presence of FR in PBT+FR+CL 30B formulations, however, does not affect their melt rheological properties.

Despite bringing about changes in melt viscosity, melting and crystallisation, the introduction of the clays, Cloisite 30B and sepiolite, does not seem to alter the thermal degradation of PBT. In terms of melting behaviour, the viscosity measurements over a temperature ramp have shown that increased viscosity in presence of nanoclay prevents dripping and flowing of polymer. In the cone calorimetric studies, this relates to shortening the time to ignition and a reduction in the rate of heat release. Furthermore, PBT formulations containing CL 30B show inhibited post-ignition combustion reactions, possibly due to physico-chemical adsorption of volatile degradation products on the surface of silicates with higher specific surface area compared to those of their sepiolite analogues.

Acknowledgements

The authors gratefully acknowledge the financial support from the European Union through the Sixth Framework Programme Priority 3 NMP “ PREDFIRE-NANO” (Contract No.: STREP 013998), and thank Dr. Andy Prike from the University of Sheffield for his help with the rheology experiments.

References

- [1] S. Bourbigot, S. Duquesne, G. Fontaine, T. Turf, S. Bellayer, in Proceedings of The Eighteenth Annual BBC Conference, Stamford, Connecticut, May 2007: 21-23.
- [2] Keszei S., Matkó Sz., Bertalan Gy., Anna P., Marosi Gy. And Tóth A., *European Polym J.* 2005,**41**, 697.
- [3] J. Tung, R.K. Gupta, G.P. Simon, G.H. Edward, S.N. Bhattacharya, *Polymer*, 2005, **46**, 10405.
- [4] A. Nohales, L. Solar, I. Porcar, C. Vallo and C.M. Gómez, *European Polym. J.*, 2006, **42**, 3093.
- [5] G.Tartaglione, D. Tabuani and G. Camino, *Microporous and Mesoporous Materials*, 2008, **107** (1-2), 161.
- [6] S.V. Levchik, E.D. Weil, *Polymer International*, 2004, **54**, 11.
- [7] S.V. Levchik, E.D. Weil, A review on thermal decomposition and combustion of thermoplastic polyesters, 2004; 15, 12: 691.
- [8] J. Zhao, A.B. Morgan, J.D. Harris, Rheological characterization of polystyrene–clay nanocomposites to compare the degree of exfoliation and dispersion, *Polymer*, 2005, **46**, 8641.
- [9] G. Broza, Z. Kwiatkowska, Roslaniec, K. Schulte, Processing and assessment of poly(butylenes terephthalate) nanocomposite reinforced with oxidised single wall carbon nanotubes, *Polymer*, 2005, **46**, 5860.
- [10] R. Wagener, T.J.G. Reisinger, *Polymer*, 2003, **44**, 7513.
- [11] F. Samyn, S. Bourbigot, C. Jama, S. Bellayer, S. Nazare, T.R. Hull, A. Castrovinci, A. Fina and G. Camino, In preparation.
- [12] F. Samyn, S. Bourbigot, C. Jama, S. Bellayer, S. Nazare, T.R. Hull, A. Castrovinci, A. Fina and G. Camino, In preparation.
- [13] X. Li, T. Kang, W. J. Cho, and C. S.Ha Lee, *Macromol. Rapid Commun*, 2001, **22**,1306.
- [14] S. Xie, S. Zhang, Wang F, Yang M, Séguéla R and Lefebvre J M, *Composites Science and Technology*, 2007,**67**, 2334.
- [15] Tian X.Y., Ruan C.J., Cui P., Liu W.T., Zheng J., Zhang X., Yao X.Y., Zheng K.and Li Y., *Chem. Eng. Comm.*, 2007,**194**,205.
- [16] J.Xiao, Y. Hu, Z .Wang, Y. Tang, Z. Chen and W. Fan, *European Polym. J.*, 2005,**41**, 1030.
- [17] B. Scharrel and T. R.Hull, *Fire and Materials*; **31** (5),327.

